Robust band gap of TiS_3 nanofilms

Jun Kang and Lin-Wang Wang*
Materials Sciences Division, Lawrence Berkeley National Laboratory, Berkeley, California 94720, United States
(Dated: May 28, 2020)

First-principles calculations are performed on the band structure of mono- and multi-layer TiS_3 nanofilms. It is found that the band gap character of TiS_3 films is quite robust, almost independent with layer thickness, vertical strain, and stacking order, which is in sharp contrast to most of other two-dimensional materials such as MoS_2. The robustness of band gap originates from the location of the CBM and VBM states, which are at the center atoms of TiS_3, thus unaffected by the layer-layer coupling. Such a property of TiS_3 nanofilms promises good application potentials in nanoelectronics and optoelectronics, and also makes TiS_3 a good platform to study electronic properties of material in 2D limit.

I. INTRODUCTION

During the past a few years, transition metal chalcogenides (TMCs) with layered structures have become a focus of research interest. MoS_2 is a typical example of TMCs, which has a direct band gap in its monolayer form.[1] MoS_2 exhibits many extraordinary physical properties such as high transistor on/off ratio,[2] photoluminescence,[3] strong exciton binding energy,[4] and valley polarization,[5] thus has great application potentials in new nanoscale devices. Following MoS_2, a great number of new elements of TMCs emerged, such as $MoSe_2$,[6] WS_2,[7] ReS_2,[8] and GaS[9]. The mechanic, electronic and optical properties of these TMCs have been extensively investigated.[10–14] So far, most of the layered TMCs under study have hexagonal (like MoS_2) or distorted hexagonal structure (like ReS_2). Nevertheless, there are also many layered TMCs with non-hexagonal symmetry, and one example is TiS_3, which has a monoclinic phase.[15,16] Very recently, triggered by its ultrahigh photoresponse (with a fast photo-current on/off switching time of 4 ms),[17] TiS_3 became a attraction of research interest. Several studies on TiS_3 have been reported. Experimentally, monolayer, few-layers, and nanoribbons of TiS_3 were successfully prepared,[17–20] and fabrication of TiS_3 based field effect transistor was achieved.[21] Strong in-plane anisotropy in the electrical and optical properties of TiS_3 was observed.[22] It was also shown that TiS_3 could be used for hydrogen evolution[23] and solid-state battery[24]. Theoretical studies showed that monolayer TiS_3 could have high carrier mobility,[25] and the band gap of TiS_3 nanoribbons was width-independent.[26]

Band gap is a key parameter for the application of materials. For two-dimensional (2D) materials, their band gap can be greatly influenced by many factors, such as layer thickness, vertical strain, and stacking order. For instance, single layer MoS_2 has a direct band gap whereas few-layer MoS_2 has a indirect gap.[27] Moreover, a semiconductor-to-metal transition can occur in bilayer MoS_2 by applying a vertical compressive strain.[28] In addition, the band gap of AA-stacked bilayer MoS_2 is 0.14 eV larger than that of AB-stacked one.[29] Therefore, it is important to understand the effects of these factors to the band gap of a new 2D material, as well as their underlaying mechanisms. In this work, using first-principles calculations, we study the effects of layer thickness, vertical strain, and stacking order on the band gap of mono- and few-layer TiS_3. In contrast to most TMCs where the hole states are at the outer layer of the structure, thus subject to many outside perturbations and make its electronic applications challenging, for TiS_3, we found that both its electron and hole states are inside the layer surface, making it robust and ideal for electronic applications.

II. COMPUTATIONAL METHODOLOGY

All the calculations are carried out using the Vienna *ab initio* simulation package (VASP)[30,31], in which the frozen-core projector augmented wave (PAW) method[32] is implemented. Both the generalized gradient approximation of Perdew-Burke-Ernzerhof (GGA-PBE)[33] and the Heyd-Scuseria-Ernzerhof (HSE06) hybrid functional[34,35] are used for exchange-correlation functional. The energy cutoff for planewave expansion is 400 eV. The k-point meshes are 7×11×1 for layers and 7×11×5 for bulk system. A vacuum layer larger than 10 Å is added between two adjacent images for layer calculations. Structural relaxation is stopped when the calculated force on each atom is smaller than 0.01 eV/Å. The van der Waals interaction is included by using the empirical correction scheme of Grimme[36].

III. RESULTS AND DISCUSSIONS

TiS_3 is composed of two-dimensional sheets stacked on the top of one another, as shown in Fig. 1, and the interactions between the sheets are van-der-Waals-like. The unitcell of a monolayer TiS_3 is a rectangle, and bulk TiS_3 has a monoclinic crystal structure. The PBE optimized lattice constants are a=4.98 Å, b=3.39 Å, and c=8.90 Å, and the lattice angle is 97.4°. These values are in good agreement with previous theoretical[25] and experimental[15] results. The interlayer binding energy of bulk TiS_3 is calculated to be 0.22 eV/unitcell.

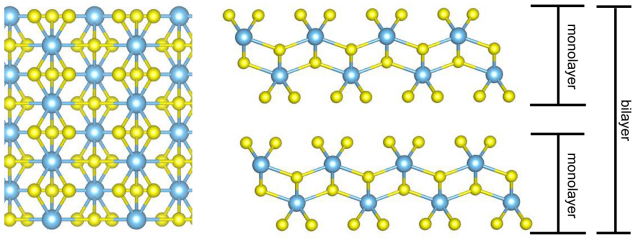

FIG. 1. (Left) Top view of a monolayer TiS_3. (Right) The side-view stacking configuration of TiS_3. Blue balls are Ti atoms, and yellow balls are S atoms.

Usually the electronic properties of layered structures strongly depend on the thickness. From monolayer to few-layers, the band structure can change a lot. For example, monolayer MoS_2 and $MoSe_2$ are direct gap semiconductors but their few-layers have indirect gap.[6,27] The interlayer binding energy for TiS_3 (0.22 eV/unitcell) is comparable to that of MoS_2 ($\sim$0.17 eV/unitcell[37]). Therefore, one may expect that the band structure of TiS_3 to show significant thickness dependence, as the case of MoS_2.

We did band structure calculations for N-layer TiS_3 with N=1-5 to explore the thickness dependence of their electronic properties. The PBE calculated band structure for monolayer TiS_3 is shown in Fig 2a. It has a direct band gap, with both conduction band minimum (CBM) and valence band maximum (VBM) at the Γ point. The band dispersion obtained by HSE06 are very similar to that by PBE, except for a enlarged band gap. The band gap calculated by PBE and HSE06 are 0.21 eV and 1.05 eV, respectively. In Fig. 2a the band plots for 2- and 5-layer TiS_3 are also presented. Interestingly, as the thickness grows, the band structure only show minor changes compared to the case of monolayer. It is found that for N=1-5, the band gaps are all direct and located at the Γ point, as shown in Fig. 2b. With increasing thickness, the band gap decreases, but the magnitude is quite small. According to PBE and HSE06 calculations, the band gap for N=5 is only 24 meV and 30 meV smaller than that of N=1, respectively. Therefore, the band gap of TiS_3 is almost independent with the layer thickness, which is very different from the case of MoS_2. The band gap of bulk TiS_3 is 0.19 eV from PBE calculation, and 1.01 eV from HSE06 calculation. Experimentally, the band gap of bulk TiS_3 is around 1 eV,[38] agrees well with the HSE06 result.

When analyzing the electronic structure of finite thickness layers, it is convenient to connect it to the bulk band structure through the zone-folding model[39,40]. Due to the weak interaction between layers, each layer in TiS_3 can be considered as a basis function. With such an simplification, an N-layer TiS_3 can be viewed as an N-atom one dimensional tight-binding chain with only nearest neighbor interaction V_0. The eigen energies of such a system is $2V_0 \sin(\frac{m\pi}{2(N+1)})$, with $m = -(N-1), -(N-3) \ldots (N-1)$. $N \to \infty$ corresponds to the bulk limit, and the eigen energies become $2V_0 \cos(k_\perp d)$, with $k_\perp$ the out-of-plane wave momenta, and d the layer-layer distance. By $2V_0 \sin(\frac{m\pi}{2(N+1)}) = 2V_0 \cos(k_\perp d)$ we have $k_\perp = \frac{(-m+N+1)\pi}{2(N+1)d}$, which are the $k_\perp$ values correspond to the eigen energies for a N-layer stack. For example, the bulk bands with $k_\perp = \frac{\pi}{2d}$ corresponds to the bands of monolayer, as shown in Fig. 3a. It is very similar to the actual band structure of monolayer in Fig. 2a.

Fig. 3b shows the HSE06 calculated eigen energies of the N highest VB (valence band) states and the N lowest CB (conduction band) states of N-layer TiS_3. According to the zone-folding model, they are mapped to the bulk bands along the $k_\perp$ direction and cross the Γ point. The Z point corresponds to $k_\perp = \frac{\pi}{d}$, and the dashed lines in Fig. 3b indicate the the corresponding $k_\perp$ for the N-layer TiS_3. The VBM and CBM of bulk TiS_3 are at the Γ and Z points, respectively. So bulk TiS_3 is an indirect gap semiconductor, as showed by previous calculations[25,41]. However, as shown in Fig. 2, few-layer TiS_3 have direct band gap. This can also be understood by the folding of bulk Brillouin zone to the 2D Brillouin zone. When the bulk band is projected to 2D Brillouin zone, the Z point also becomes Γ, this makes the system direct with a nonzero oscillator strength between the VBM and CBM states. It is seen from Fig. 3b that the actual eigen energies of the few-layer TiS_3 match well with the bulk band structure, and the accuracy of the zone-folding model increases as the layer thickness increases (namely the system is more bulk-like). For 1-, 2-, and 5-layer TiS_3, the band gap errors of the zone-folding model are 21 meV, 12 meV, and 5 meV, respectively.

Fig. 3b shows that the zone-folding model can be used to predict the eigen energies of finite thickness layer systems from bulk band structure. It also shows that the interlayer coupling strength V_0 for VBM and CBM are really small. We fitted the bulk bands in Fig. 3b into the function $2V_0 \cos(k_\perp d) + E_0$, and found that the V_0 is 28 meV for CB, and only 4 meV for VB. The weak coupling leads to a small bulk band dispersion and therefore a small difference between the band gaps of monolayer and the bulk limit. As a result, the change of band gap, as well as the band offset, is only in the order of several tens of meV when increasing the thickness of TiS_3.

To understand the origin of the small coupling constants, we have calculated the partial charge density of the CBM and VBM states of monolayer TiS_3, as shown in Fig. 3c. Both the charge densities of CBM and VBM are distributed inside the layer, and the surface S atoms have no contribution to them. Such distributions minimize the interlayer CBM or VBM overlapping when the monolayers are stacked together, leading to small coupling constants. It is also seen that the CBM is more extended along the out-of-plane direction than the VBM. This leads to stronger interlayer CBM coupling than that of VBM as indicated by the above calculated V_0, and the

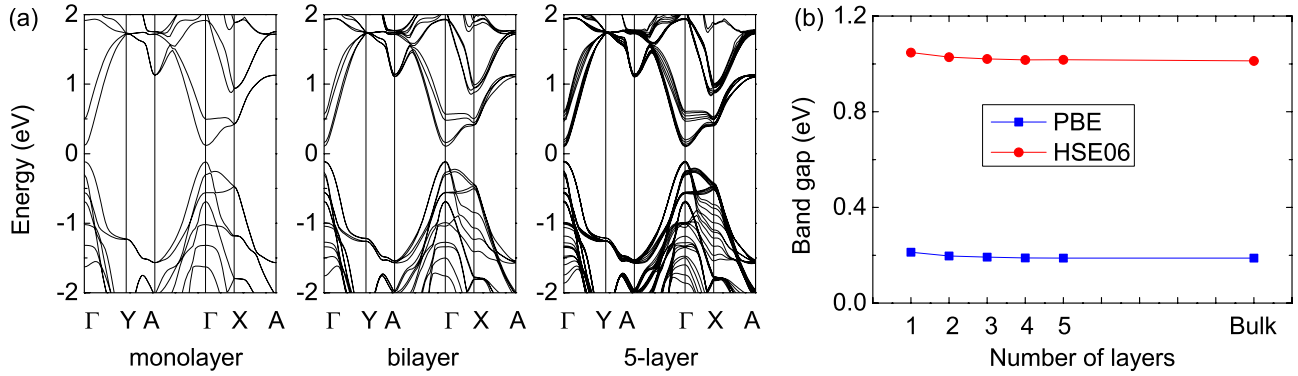

FIG. 2. (a) PBE calculated band structure and (b) band gap values of TiS_3 with different layer thickness.

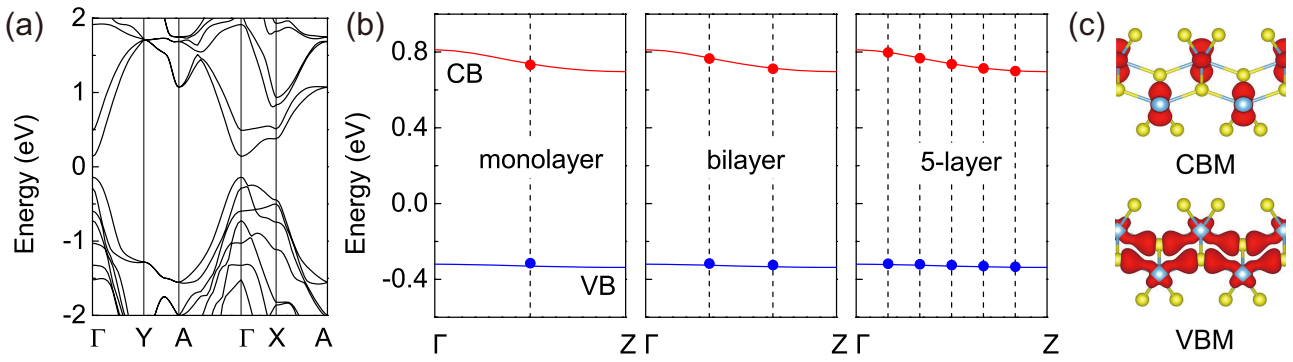

FIG. 3. (a) PBE calculated band structure of bulk TiS_3 on the 2D Brillouin zone slice perpendicular to the the $k_\perp$ direction and across $k_\perp = \frac{\pi}{2d}$. (b) The HSE06 calculated eigen energies (solid circles) of the N highest VB states and the N lowest CB states of a N-layer TiS_3. They are mapped into the bulk bands (solid lines) of TiS_3 along the $k_\perp$ direction and cross the Γ point. The dashed lines indicate the corresponding $k_\perp$ for the N-layer TiS_3. (c) The charge distribution of the VBM and CBM states of monolayer TiS_3.

bulk CB exhibits more dispersion than VB, as shown in Fig. 3b.

Besides layer thickness, typically the electronic structures of 2D materials are sensitive to many other factors, such as vertical strain and stacking order.[28,29] In the following we examine the response of band gap of few-layer TiS_3 to vertical strain and stacking order. Vertical compressive strain were applied to TiS_3 with 2-5 layers by changing the interlayer distance. The variation of band gap with the strain is given in Fig. 4a. All structures shows almost identical behavior, regardless of the thickness. The band gap is insensitive to the compressive strain. When the strain increases from 0 to 6.8 %, both PBE and HSE06 calculations indicate that the band gaps only slightly increase by about 70 meV, and remain direct at the Γ point. To study the effect of stacking order on the band gap, we have taken a bilayer TiS_3 as an example. Starting from the equilibrium stacking configuration, the two TiS_3 layers were relatively shifted with different displacements and along three different directions a, b, and ab to realize different stacking configuration. The band gap as a function of the in-plane translation is presented in Fig. 4b. Again, the band gap remains direct, and is insensitive to the in-plane translation, namely the stacking order. Both PBE and HSE06 calculations indicates the maximum change in band gap is only about 40 meV. The small effects of vertical strain and stacking order on the band gap of TiS_3 can also be understood by the wavefunction characters of its CBM and VBM. Because the CBM and VBM are distributed inside the layers, even with decreased layer distance or change of stacking order, the interlayer coupling between CBM or VBM is still weak, thus the band gap is almost intact. Note that in-plane strain can greatly influence the CBM and VBM. So the band gap of TiS_3 can be tuned by applying in-plane strain.[42,43]

The above results indicate that TiS_3 has robust CBM and VBM states, and band gap, which is insensitive to layer thickness, vertical strain, and stacking order. In contrast, these factors have great effects on the band gap of many other 2D materials such as MoS_2. The protected nature of CBM and VBM in TiS_3 makes it a good candidate for electronic devices where its internal electronic structure and transport properties will not be affected by additional depositions (e.g, gate and source and drain electrodes). The vertical strain resistance can make the device stable against thermal expansion and mechanical deformation. In addition, the band gap value of ∼1 eV

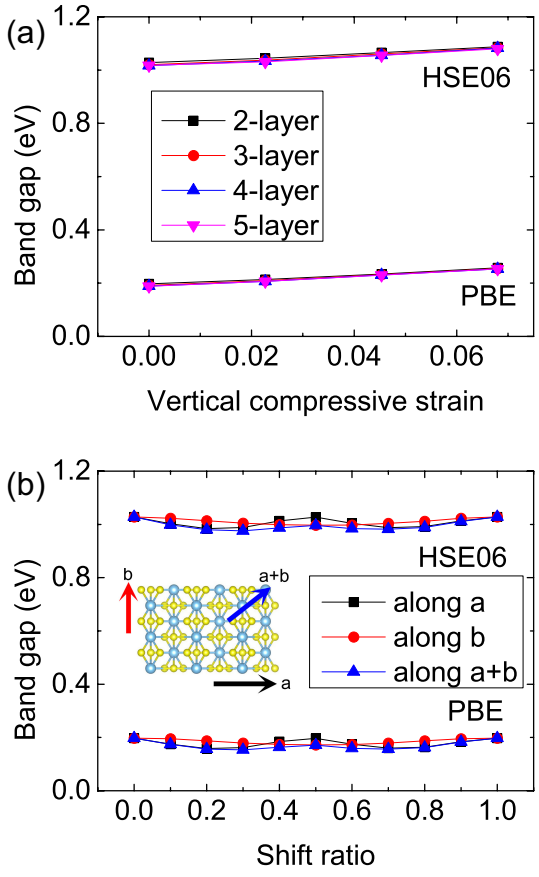

FIG. 4. (a) Band gap values of TiS_3 with vertical compressive strain. (b) Band gap of bilayer TiS_3 as a function of relative in-plane translation along three different directions. The shifting ratio is the displacement divided by the lattice constant along that direction.

is favorable for adsorption of visible light, making TiS_3 a good candidate for optoelectronic applications. Moreover, TiS_3 can be a good platform to study electronic properties in 2D limit since the layer-decoupled character of its CBM and VBM states enables one explore 2D-like system without the need of monolayer.

IV. CONCLUSIONS

In summary, we have performed first-principles calculations on the band structure of mono- and few-layer TiS_3 films. All films studied exhibit a ∼1 eV direct band gap at the Γ point. It is found that the band gap of TiS_3 films is quite robust, almost independent with layer thickness, vertical strain, and stacking order. This property originates from the protected nature of the CBM and VBM states inside the layer. The robust band gap of TiS_3 nanofilm promises good application potentials in nanoelectronics and optoelectronics, and also makes it a good platform to study electronic properties of material in 2D limit.

ACKNOWLEDGMENTS

This work was supported by the Director, Office of Science, the Office of Basic Energy Sciences (BES), Materials Sciences and Engineering (MSE) Division of the U.S. Department of Energy (DOE) through the organic/inorganic nanocomposite program under contract DE-AC02-05CH11231. It used resources of the National Energy Research Scientific Computing Center.

* lwwang@lbl.gov

[1] K. F. Mak, C. Lee, J. Hone, J. Shan, and T. F. Heinz, Phys. Rev. Lett. **105**, 136805 (2010).
[2] B. Radisavljevic, A. Radenovic, J. Brivio, V. Giacometti, and A. Kis, Nat. Nanotechnol. **6**, 147 (2011).
[3] A. Splendiani, L. Sun, Y. Zhang, T. Li, J. Kim, C.-Y. Chim, G. Galli, and F. Wang, Nano Lett. **10**, 1271 (2010).
[4] A. Ramasubramaniam, Phys. Rev. B **86**, 115409 (2012).
[5] T. Cao, G. Wang, W. Han, H. Ye, C. Zhu, J. Shi, Q. Niu, P. Tan, E. Wang, B. Liu, and J. Feng, Nat. Commun. **3**, 887 (2012).
[6] S. Tongay, J. Zhou, C. Ataca, K. Lo, T. S. Matthews, J. Li, J. C. Grossman, and J. Wu, Nano Lett. **12**, 5576 (2012).
[7] T. Georgiou, R. Jalil, B. D. Belle, L. Britnell, R. V. Gorbachev, S. V. Morozov, Y.-J. Kim, A. Gholinia, S. J. Haigh, O. Makarovsky, L. Eaves, L. A. Ponomarenko, A. K. Geim, K. S. Novoselov, and A. Mishchenko, Nat. Nanotechnol. **8**, 100 (2013).
[8] S. Tongay, H. Sahin, C. Ko, A. Luce, W. Fan, K. Liu, J. Zhou, Y.-S. Huang, C.-H. Ho, J. Yan, D. F. Ogletree, S. Aloni, J. Ji, S. Li, J. Li, F. M. Peeters, and J. Wu, Nat. Commun. **5**, 3252 (2014).
[9] D. J. Late, B. Liu, J. Luo, A. Yan, H. Matte, M. Grayson, C. Rao, and V. P. Dravid, Adv. Mater. **24**, 3549 (2012).
[10] Q. H. Wang, K. Kalantar-Zadeh, A. Kis, J. N. Coleman, and M. S. Strano, Nat. Nanotechnol. **7**, 699 (2012).
[11] C. Ataca, H. Şahin, and S. Ciraci, J. Phys. Chem. C **116**, 8983 (2012).
[12] K. Liu, Q. Yan, M. Chen, W. Fan, Y. Sun, J. Suh, D. Fu, S. Lee, J. Zhou, S. Tongay, J. Ji, J. B. Neaton, and J. Wu, Nano lett. **14**, 5097 (2014).
[13] D. A. Chenet, O. B. Aslan, P. Y. Huang, C. Fan, A. M. van der Zande, T. F. Heinz, and J. C. Hone, Nano lett. **15**, 5667 (2015).
[14] S. Yang, Y. Li, X. Wang, N. Huo, J.-B. Xia, S.-S. Li, and J. Li, Nanoscale **6**, 2582 (2014).
[15] L. Brattas and A. Kjekshus, Acta Chem. Scand. **26**, 3441 (1972).
[16] S. Furuseth, L. Brattas, and A. Kjekshus, Acta Chem. Scand. **29**, 623 (1975).
[17] J. O. Island, M. Buscema, M. Barawi, J. M. Clamagirand, J. R. Ares, C. Sánchez, I. J. Ferrer, G. A. Steele, H. S. J. van der Zant, and A. Castellanos-Gomez, Adv. Optic. Mater. **2**, 641 (2014), ISSN 2195-1071.

[18] J. O. Island, M. Barawi, R. Biele, A. Almazán, J. M. Clamagirand, J. R. Ares, C. Sánchez, H. S. van der Zant, J. V. Álvarez, R. D'Agosta, I. J. Ferrer, and A. Castellanos-Gomez, Adv. Mater. **27**, 2595 (2015).

[19] A. S. Pawbake, J. O. Island, E. Flores, J. R. Ares, C. Sanchez, I. J. Ferrer, S. R. Jadkar, H. S. van der Zant, A. Castellanos-Gomez, and D. J. Late, ACS Appl. Mater. Interfaces **7**, 24185 (2015).

[20] A. J. Molina-Mendoza, M. Barawi, R. Biele, E. Flores, J. R. Ares, C. Sánchez, G. Rubio-Bollinger, N. Agraït, R. D'Agosta, I. J. Ferrer, and A. Castellanos-Gomez, Adv. Electron. Mater. **1**, 1500126 (2015).

[21] A. Lipatov, P. M. Wilson, M. Shekhirev, J. D. Teeter, R. Netusil, and A. Sinitskii, Nanoscale **7**, 12291 (2015).

[22] J. O. Island, R. Biele, M. Barawi, J. M. Clamagirand, J. R. Ares, C. Sanchez, H. S. van der Zant, I. J. Ferrer, R. D'Agosta, and A. Castellanos-Gomez, arXiv preprint arXiv:1510.06889(2015).

[23] M. Barawi, E. Flores, I. Ferrer, J. Ares, and C. Sánchez, J. Mater. Chem. A **3**, 7959 (2015).

[24] N. Tanibata, T. Matsuyama, A. Hayashi, and M. Tatsumisago, J. Power Sources **275**, 284 (2015).

[25] J. Dai and X. C. Zeng, Angew. Chem. Int. Ed. **54**, 7572 (2015).

[26] J. Kang, H. Sahin, H. D. Ozaydin, R. T. Senger, and F. m. c. M. Peeters, Phys. Rev. B **92**, 075413 (2015).

[27] W. S. Yun, S. W. Han, S. C. Hong, I. G. Kim, and J. D. Lee, Phys. Rev. B **85**, 033305 (2012).

[28] S. Bhattacharyya and A. K. Singh, Phys. Rev. B **86**, 075454 (2012).

[29] J. He, K. Hummer, and C. Franchini, Phys. Rev. B **89**, 075409 (2014).

[30] G. Kresse and J. Hafner, Phys. Rev. B **47**, 558 (1993).

[31] G. Kresse and J. Furthmüller, Phys. Rev. B **54**, 11169 (1996).

[32] G. Kresse and D. Joubert, Phys. Rev. B **59**, 1758 (1999).

[33] J. P. Perdew, K. Burke, and M. Ernzerhof, Phys. Rev. Lett. **77**, 3865 (1996).

[34] J. Heyd, G. E. Scuseria, and M. Ernzerhof, J. Chem. Phys. **118**, 8207 (2003).

[35] A. V. Krukau, O. A. Vydrov, A. F. Izmaylov, and G. E. Scuseria, J. Chem. Phys. **125**, 224106 (2006).

[36] S. Grimme, J. Comput. Chem. **27**, 1787 (2006).

[37] T. Björkman, A. Gulans, A. V. Krasheninnikov, and R. M. Nieminen, Phys. Rev. Lett. **108**, 235502 (2012).

[38] I. Ferrer, J. Ares, J. Clamagirand, M. Barawi, and C. Sánchez, Thin Solid Films **535**, 398 (2013).

[39] M. Koshino and T. Ando, Phys. Rev. B **76**, 085425 (2007).

[40] K. F. Mak, M. Y. Sfeir, J. A. Misewich, and T. F. Heinz, Proc. Natl. Acad. Sci. U.S.A **107**, 14999 (2010).

[41] Y. Jin, X. Li, and J. Yang, Phys. Chem. Chem. Phys. **17**, 18665 (2015).

[42] J. Kang, H. Sahin, and F. M. Peeters, Phys. Chem. Chem. Phys. **17**, 27742 (2015).

[43] M. Li, J. Dai, and X. C. Zeng, Nanoscale **7**, 15385 (2015).